GEOPHYSICAL RESEARCH LETTERS, VOL. 22, NO. 6, PAGES 683-686, MARCH 15, 1995

TOMS total ozone trends in potential vorticity coordinates

William J. Randel and Fei Wu

National Center for Atmospheric Research, P. O. Box 3000, Boulder, CO 80307

Abstract. Global total ozone measurements from the Nimbus 7 Total Ozone Mapping Spectrometer (TOMS) are analyzed using potential vorticity (PV) as an approximate vortex-following coordinate. We analyze the time period November 1978-May 1991, prior to the volcanic eruption of Mt. Pinatubo. The TOMS data are remapped into PV coordinates and trends are calculated, thereby characterizing ozone losses inside and outside the winter polar vortices. These analyses show large regions of ozone loss outside of the vortex in both hemispheres. Furthermore, these data suggest that midlatitude losses in the NH during winter-spring do not result solely from the transport of ozone depleted air from inside to outside the vortex.

Introduction

Decreases in global ozone amounts have been detected over the last two decades by a variety of ground- and satellite-based measurement techniques [*WMO*, 1991; *Stolarski et al.*, 1992]. One instrument that was particularly useful for trend detection was the Total Ozone Mapping Spectrometer (TOMS) on Nimbus 7, which provided nearly global maps of column ozone on a daily basis from November 1978 until early May 1993. *Stolarski et al.* [1991] used these TOMS data to document global ozone losses of approximately -2.6% per decade; these losses were largest over NH midlatitudes (30°-60°N) during winter-spring and over the high latitude SH throughout the year (maximizing in September-October), with near zero trends in low latitudes. One of the more interesting questions arising from that study was the origin of the NH midlatitude ozone losses: did such losses originate inside the polar vortex and get transported to midlatitudes, or was in situ chemical ozone depletion occurring outside the vortex? These questions were somewhat confused by the zonal averaging applied to the TOMS data in *Stolarski et al.* [1991]; the vortex is often displaced substantially off the pole in the NH winter stratosphere, so that zonal averaging may confuse inside versus outside vortex processes.

The focus of this study is to analyze these TOMS data using potential vorticity (PV) as an approximate vortex-following coordinate. Our motivation is to characterize the space-time signatures of observed ozone loss in relation to the structure of the polar vortex. Potential vorticity derived from National Meteorological Center (NMC) operational stratospheric analyses is used to define the vortex structure [*McIntyre and Palmer*, 1982; *Buchart and Remsberg*, 1986; *Schoeberl et al.*, 1989, 1992; *Norton*, 1994], and the TOMS data averaged in PV coordinates are subjected to trend analyses as in *Stolarski et al.* [1991].

Data and Analyses

In this work we analyze column ozone from Version 6 of the Nimbus 7 TOMS data, covering November 1978-May 1991. We have excluded data beyond this time because of the large ozone depletions observed during NH winters 1991-92 and 1992-93 [*Gleason et al.*, 1993; *Bojkov et al.*, 1993; *Kerr et al.*, 1993; *Komhyr et al.*, 1994], likely associated with effects of the Mt. Pinatubo volcanic eruption in June 1991.

Potential vorticity (PV) is calculated from daily wind and temperature fields derived from National Meteorological Center (NMC) operational stratospheric analyses, and results are interpolated to isentropic (constant potential temperature) surfaces. PV is given by

$$PV = -g(\zeta + f)\frac{\partial \theta}{\partial p} \quad ,$$

using standard notation [e.g., *Butchart and Remsberg*, 1986]. Both the TOMS and PV data are sampled on 5° latitude by 10° longitude grids. As an example, Figure 1a shows PV on the 520 K isentropic surface (near 21 km and near the 50 mb pressure level) for 15 March 1986. We have chosen the 520 K isentrope for the analyses of TOMS data because this altitude (21 km) is near the density weighted ozone mixing ratio maximum, and hence near the largest contribution to column ozone; the results here are not sensitive to the exact isentropic level used. The PV field in Figure 1a shows a slightly elongated polar vortex displaced off the pole towards Asia; the PV structure on this day exhibits the typical structure of relatively weak gradients over midlatitudes (the 'surf zone'), a strong gradient region identifying the vortex edge, and weaker gradients in the vortex interior. Figure 1b shows the corresponding total ozone field for 15 March 1986, with three of the PV contours from Figure 1a superimposed. The middle PV contour is the calculated vortex edge (maximum PV gradient), while the inner and outer contours define the vortex edge boundary region (region of strongest PV gradient); these are calculated using the objective criteria described in *Nash et al.* [1994]. One feature immediately evident in Figure 1b is that maximum total ozone values occur outside or near the edge of the vortex, while there is a pronounced minimum near the vortex center. The result of this structure is that when averages are calculated around contours of constant PV, total ozone exhibits a distinct minimum inside the vortex, whereas the zonal average exhibits monotonic increase towards the pole. This result is clearly shown in Figure 2, which compares zonal averages versus PV-averages of the data shown in Figure 1b (the PV-averaged results are plotted as a function of equivalent latitude of the area inside the individual PV contours). A further advantage to using PV-coordinates occurs during midwinter, when TOMS data are unavailable over polar night regions: for situations when the vortex is displaced away from the pole, the PV-averaged results extend to higher equivalent latitudes than those available using zonal mean data.

In order to calculate the monthly mean data used here, daily TOMS and PV data are used to map the TOMS data to PV coordinates, and averages along PV contours are calculated. These daily data are transformed to equivalent latitude based on the PV fields, and then monthly averages are calculated (using at least five days of data for each month). The resulting seasonal cycle of TOMS ozone is shown in Figure 3, derived from the

Paper number 94GL02790
0094-8534/95/94GL-02790$03.00

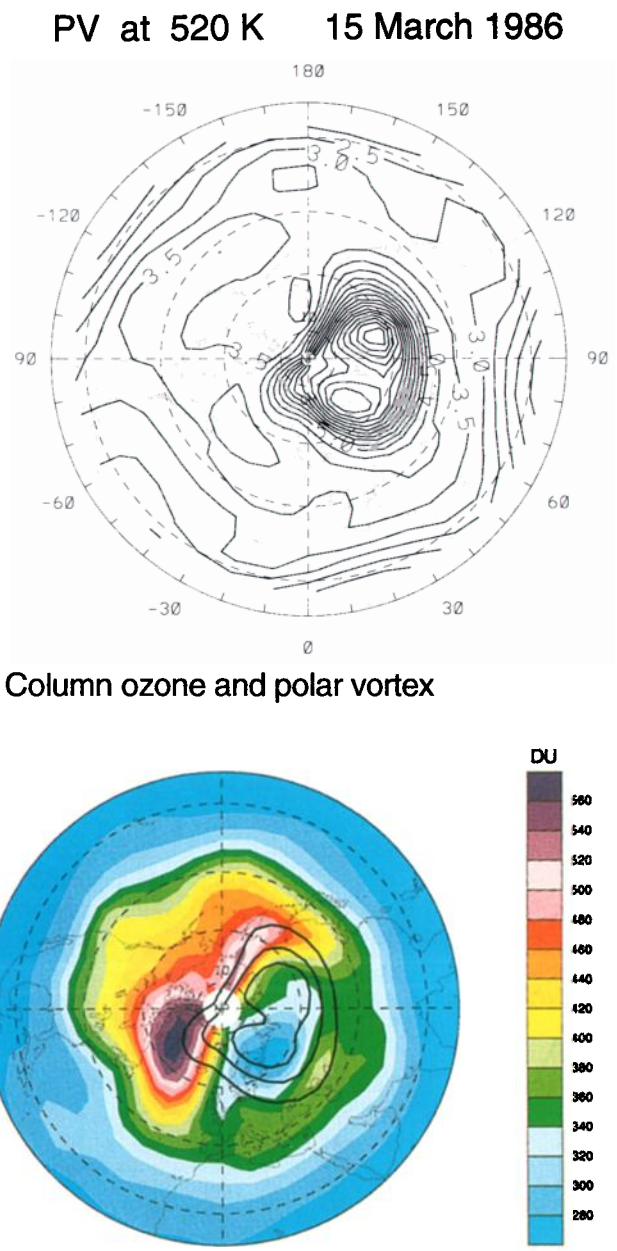

Figure 1. (a-top) 16 March 1986 potential vorticity (PV) on the 520 K potential temperature surface. Units are 10^{-5} K m^2 kg^{-1} s^{-1}. (b-bottom) 16 March 1986 TOMS total ozone in Dobson units. The three heavy lines denote the vortex edge and boundary region derived from the PV map above.

(almost) 13 years of data analyzed here. Included in Figure 3 are lines denoting the climatological vortex edge and boundary region for each winter month, derived from histograms of these quantities obtained from daily data. The seasonal cycle in Figure 3 shows a column ozone maximum slightly equatorward of the edge of the vortex during NH winter-spring, qualitatively similar to the maximum observed in SH winter-spring (which is also slightly equatorward of the vortex edge in these analyses). This total ozone maximum near the vortex edge is in agreement with the PV-coordinate analyses of aircraft data in *Schoeberl et al.* [1992], their Plate 2, and is consistent with strongest downward velocities in the lower stratosphere near the vortex edge, rather than in the vortex center [*Mahlman et al.*, 1980; *Schoeberl et al.*, 1992; *Manney et al.*, 1994]. We note that zonal averages of TOMS data [i.e., *Bowman and Krueger*, 1985] do not reveal this structure in the NH, due to asymmetry of the vortex.

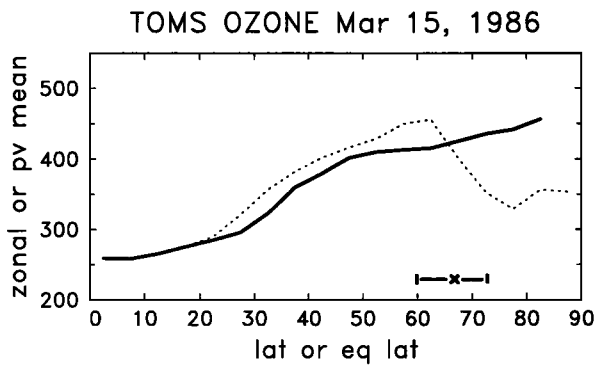

Figure 2. Latitudinal structure of TOMS ozone on 16 March 1994 (Figure 1b), calculated from the zonal average (solid line) and from averages around contours of constant PV (dashed lines). The PV averages have been plotted here using the equivalent latitude of the individual PV contours. The bracketed x denotes the equivalent latitudes of the vortex edge and boundary region calculated for this day (heavy contours shown in Figure 1b).

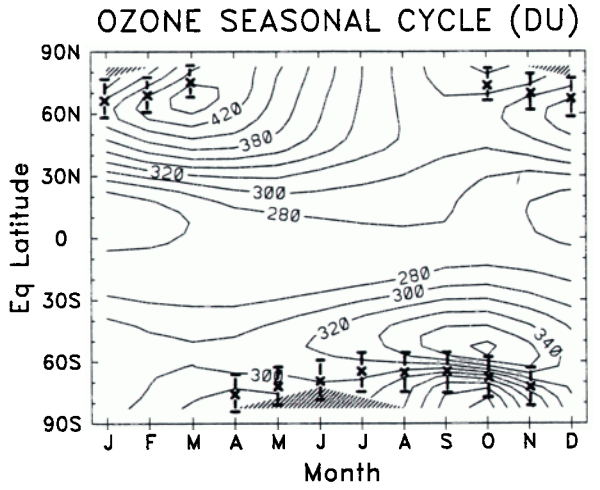

Figure 3. TOMS total ozone seasonal cycle constructed in PV coordinates (transformed to equivalent latitude). The bracketed x's denote the statistical vortex edge and boundary regions for each winter month, constructed from histograms of daily statistics.

Trends

Total ozone trends are estimated here using a seasonally-varying linear regression analysis applied to the monthly mean data. The statistical model includes linear trend, solar cycle, quasi-biennial oscillation (QBO) and El Nino-Southern Oscillation (ENSO) effects, and residuals are modeled as first order auto-regressive; the calculations follow those in *Randel and Cobb*, 1994. Error estimates include a 0.13% per year instrumental trend error [*Stolarski et al.*, 1991]. Figure 4 shows the resulting trends versus month and equivalent latitude. Shading in Figure 4 indicates that the calculated trend is not different from zero at the 2σ level, and lines are also included in Figure 4 indicating the climatological vortex edge and boundary position for each winter month (as in Figure 3).

The ozone trends shown in Figure 4 are similar to the zonal mean results presented in *Stolarski et al.*, 1991, but our calculations clearly separate trends with respect to location of the polar vortices. Results in Figure 4 show significant negative trends outside of the vortex throughout the year in the SH. These year-round losses outside the SH vortex are likely due at least in part to transport of ozone depleted air out of the Antarctic ozone hole into midlatitudes following vortex breakdown, which then

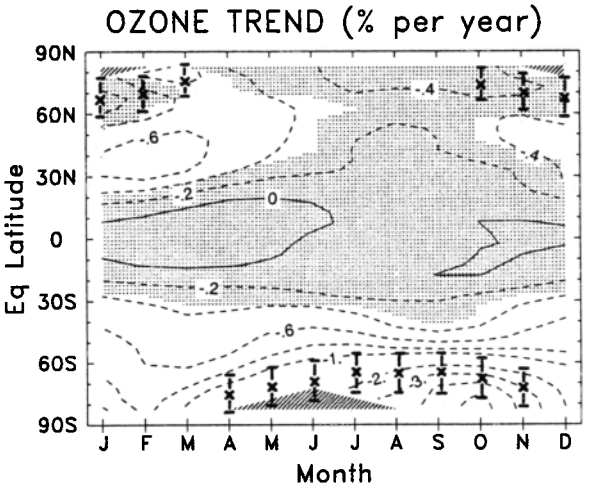

Figure 4. TOMS total ozone linear trends calculated from data averaged in PV coordinates (transformed to equivalent latitude); contours are 0, -.2, -.4, ..., -1., -2., -3., ... percent per year. Shaded regions denote where the statistical trends are not different from zero at the 2σ level. Bracketed x's denote the statistical vortex edge and boundary region for each winter month.

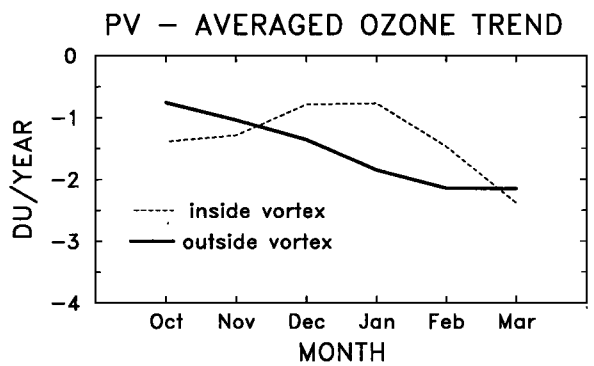

Figure 5. TOMS total ozone trends during NH winter-spring (in units of Dobson units per year), averaged over regions inside and outside of the outer vortex boundary (shown in Figures 3-4 and listed in Table 1). One sigma uncertainty levels for these trends are of order 0.7 and 0.35 DU/year inside and outside the vortex, respectively.

persists into following years [*Sze et al.*, 1989; *Prather et al.*, 1990; *Malhman et al.*, 1994]. Figure 4 also shows significant ozone losses outside of the vortex in the NH during winter-spring; these are much more seasonally dependent and less persistent into summer than the midlatitude depletions seen in the SH (suggesting less interannual 'memory' in the NH). The trend magnitudes over NH midlatitudes derived here are approximately 20% lower than the zonal mean results in *Stolarski et al.* [1991], whereas our results in SH spring are somewhat higher. Direct comparisons of PV-averaged versus zonal mean data show a reduction in interannual variance and smaller trend uncertainties for the PV analyses; this implies that part of the interannual variability in zonal mean data is an artifact related to vortex variability.

Figure 5 shows ozone losses averaged over equivalent latitude bands inside and outside of the vortex during NH winter-spring, calculated in Dobson units (DU) per year rather than percent per year. Outside vortex values are averaged over 30° to the outer vortex boundary (shown in Figures 3-4, and tabulated in Table 1), while inside values are averaged from this outer boundary to 85°N. Inside vortex trends reach a minimum in midwinter (December-January), consistent with a lack of sunlight during midwinter required for chemical ozone depletion. Conversely, the outside vortex trends increase steadily in time throughout winter-spring.

Given the current understanding of ozone depletion in NH middle-high latitudes in winter, there are three possible causes for the observed ozone losses outside of the vortex seen in Figures 4-5: 1) ozone may be depleted inside the vortex [due to polar stratospheric cloud (PSC) induced chemical reactions, e.g., *Webster et al.*, 1993], and the ozone depleted air then transported to midlatitudes [see the SH example in *Adkinson et al.*, 1989]; 2) vortex air may be chemically processed, then mixed to midlatitudes, where in-situ ozone depletion occurs [*Tuck et al.*, 1992; *Norton and Chipperfield*, 1994]; or 3) midlatitude ozone loss may occur independently of (or in addition to) vortex-asssociated PSC processes [possibly associated with midlatitude sulfate aerosols; *Hofmann and Solomon*, 1989]. Given the TOMS observations of ozone loss inside and outside the vortex (Figure 5), and knowledge of the vortex area, we can quantitatively assess the cross-vortex exchange rates necessary for mechanism (1) to account solely for the observed midlatitude trend increase between early winter and spring. This exchange rate is estimated from mass continuity via:

$$\frac{\partial}{\partial t}\left[\text{O}_3 \text{ trends outside vortex}\right] = \left[\text{O}_3 \text{ trends inside vortex}\right] \cdot \left[\frac{\text{area inside vortex}}{\text{area outside vortex}}\right] \cdot \left[\text{exchange rate}\right]. \quad (1)$$

Table 1 tabulates the exchange rates calculated from Eq. 1 and the data in Figure 5, and shows that the entire volume of vortex air must be flushed to midlatitudes 1-2 times per month in midwinter for transport of ozone depleted air to account solely for the observed seasonal increase in midlatitude ozone depletion (although these estimates should be viewed qualitatively in light of the uncertainties associated with trend estimates and time derivatives). This rate of exchange is substantially larger than calculations based on horizontal mass flux estimates [*Waugh et al.*, 1994; *Dahlberg and Bowman*, 1994], inferred from mean vertical velocities [*Schoeberl et al.*, 1992], or derived from three-dimensional trajectory calculations [*Manney et al.*, 1994]. Our conclusion is that the outside vortex ozone losses seen in TOMS data occur by processes other than mechanism (1) above.

Summary

The motivation for the PV-based analyses here is to study ozone trends referenced with respect to a vortex-based coordinate system. This method of averaging around PV contours is more physically meaningful than zonal averaging, and in fact part of

Table 1. Vortex exchange rates estimated from ozone trends (Eq. 1).

Month	Vortex Outer Boundary	$\frac{\partial}{\partial t}$(Outside Trend) (Du/Year/Month)	Inside Trend (Du/Year)	$\left(\frac{\text{Inside Area}}{\text{Outside Area}}\right)$	Exchange Rate (1/Month)
Nov.	61.3°	-.30	-1.29	.27	0.9
Dec.	58.3°	-.41	-0.79	.35	1.5
Jan.	57.6°	-.39	-0.77	.37	1.4
Feb.	59.8°	-.15	-1.47	.31	0.3

the interannual variability in zonal average data is removed when the data are studied in PV coordinates. The trend analyses (Figure 4) shows ozone losses outside of the vortex for both hemispheres; midlatitude losses occur year-round in the SH, but only during winter-spring in the NH. The trends inside the vortex in the NH exhibit a minimum in midwinter (during polar night), whereas those outside the NH vortex increase in time throughout winter-spring. We have used that temporal increase outside the vortex to estimate the mass flow rate that would be necessary if these losses occurred inside the vortex and were subsequently transported to midlatitudes. The results (Table 1) suggest exchange rates of 1-2 vortex volumes per month in midwinter, substantially larger than independent estimates of vortex flow rates (referenced above). We thus conclude that the midlatitude losses occur due to in situ midlatitude processes, possibly associated with vortex processed air transported to midlatitudes or reactions associated with background sulfate aerosols. This latter mechanism is also suggested by the observed ozone losses in the NH during early winter (November-December) in Figure 4; these appear well before the occurrence of PSC threshold temperatures at high latitudes.

Acknowledgments. The authors thank Bill Mankin and Mike Coffey for helpful discussions. Comments by Jerry Mahlman, Mark Schoeberl, Susan Solomon, and two anonymous reviewers led to substantial improvements in this paper. Marilena Stone expertly prepared the manuscript. This work has been supported under NASA grants W-16215 and W-18181, and NOAA grant NAAZ0000300149. National Center for Atmospheric Research is sponsored by the National Science Foundation.

References

Atkinson, R. J., W. A. Matthews, P. A. Newman and R. A. Plumb, Evidence of the mid-latitude impact of Antarctic ozone depletion, *Nature, 340,* 290-293, 1989.

Bojkov, R. D., C. S. Zerefos, D. S. Balis, I. C. Ziomas and A. F. Bais, Record low total ozone during Northern winters of 1992 and 1993, *Geophys. Res. Lett., 20,* 1351-1354, 1993.

Bowman, K. P. and A. J. Krueger, A global climatology of total ozone from the Nimbus 7 total ozone mapping spectrometer, J. *Geophys. Res., 90,* 7967-7976, 1985.

Butchart, N. and E. E. Remsberg, The area of the stratospheric polar vortex as a diagnostic for tracer transport on an isentropic surface, *J. Atmos. Sci., 43,* 1379-1405, 1986.

Dahlberg, S. P. and K. P. Bowman, Climatology of large-scale isentropic mixing in the Arctic winter stratosphere from analyzed winds, *J. Geophys. Res.*, in press, 1994.

Gleason, J. F., et al., Record low global ozone in 1992, *Science, 260,* 523-526, 1993.

Hofmann, D. and S. Solomon, Ozone destruction through heterogeneous chemistry following the eruption of El Chichon, *J. Geophys. Res., 94,* 5029-5041, 1989.

Kerr, J. B., D. I. Wardle and D. W. Tarasick, Record low ozone values over Canada in early 1993, *Geophys. Res. Lett., 20,* 1979-1982, 1993.

Komhyr, W. D., R. D. Grass, R. D. Evans, R. K. Leonard, D. M. Quincy, D. J. Hofmann and G. L. Koenig, Unprecedented 1993 ozone decrease over the United States from Dobson spectrophotometer observations, *Geophys. Res. Lett., 21,* 210-214, 1994.

McIntyre, M. E. and T. N. Palmer, Breaking planetary waves in the stratosphere, *Nature, 305,* 593-600, 1983.

Mahlman, J. D. and L. J. Umscheid, Three-dimensional tracer structure and behavior as simulated in two ozone precursor experiments, *J. Atmos. Sci., 37,* 655-685, 1980.

Mahlman, J. D., J. P. Pinto and L. J. Umscheid, Transport, radiative and dynamical effects of the Antarcic ozone hole: A GFDL 'SKYHI' model experiment, *J. Atmos. Sci., 51,* 489-508, 1994.

Manney, G. L., R. W. Zurek, A. O'Neill and R. Swinbank, On the motion of air through the stratospheric polar vortex, *J. Atmos. Sci., 51,* 2973-2994, 1994.

Nash, E. R., P. A. Newman, J. E. Rosenfield and M. R. Schoeberl, An objective determination of the polar vortex using Ertel's potential vorticity, *J. Geophys. Res.*, in press, 1994.

Norton, W. A., Breaking Rossby waves in a model stratosphere diagnozed by a vortex following coordinate system and a technique for advecting material contours, *J. Atmos. Sci., 51,* 654-673, 1994.

Norton, W. A. and M. P. Chipperfield, Quantification of the transport of chemically activated air from the northern hemisphere polar vortex, *J. Geophys. Res.*, submitted, 1994.

Prather, M., M. M. Garcia, R. Suozzo and D. Rind, Global impact of the Antarctic ozone hole: dynamical dilution with a three-dimensional chemical transport model, *J. Geophys. Res., 95,* 3449-3471, 1990.

Randel, W. J. and J. B. Cobb, Coherent variations of monthly mean total ozone and lower stratospheric temperature, *J. Geophys. Res., 99,* 5433-5447, 1994.

Schoeberl, M. R., et al., Reconstruction of the constituent distribution and trends in the Antarctic polar vortex from ER-2 flight observations, J. Geophys. Res., *94,* 16,815-16,846, 1989.

Schoeberl, M. R., L. R. Lait, P. A. Newman and J. E. Rosenfield, The structure of the polar vortex, *J. Geophys. Res., 97,* 7859-7882, 1992.

Stolarski, R. S., P. Bloomfield, R. D. McPeters and J. R. Herman, Total ozone trends deduced from Nimbus 7 TOMS data, *Geophys. Res. Lett., 18,* 1,015-1,018, 1991.

Stolarski, R. S., R. Bojkov, L. Bishop, C. Zerefos, J. Staehdin and J. Zawodny, Measured trends in stratospheric ozone, *Science, 256,* 342-349, 1992.

Sze, N. D., et al., Antarctic ozone hole: Possible implications for ozone trends in the Southern Hemisphere, *J. Geophys. Res., 94,* 11521-11528, 1989.

Tuck, A. F., et al., Polar stratospheric cloud processed air and potential vorticity in the Northern Hemisphere lower stratosphere at mid-latitudes during winter, *J. Geophys. Res., 97,* 7883-7904, 1992.

Waugh, D. W., et al., Transport out of the lower stratospheric Arctic vortex by Rossby wave breaking, *J. Geophys. Res., 99,* 1071-1088, 1994.

Webster, C. R., et al., Chlorine chemistry on polar stratospheric cloud particles in the Arctic winter, *Science, 261,* 1130-1134, 1993.

World Meteorological Organization, Scientific Assessment of Ozone Depletion: 1991, WMO Global Ozone Research and Monitoring Project, *Report No. 25,* 1991.

W. Randel and F. Wu, Atmospheric Chemistry Division, National Center for Atmospheric Research, P. O. Box 3000, Boulder, CO 80307

(Received June 7, 1994; accepted July 12, 1994)